

MULTISTAGE TURBINE SOUND GENERATION AND PROPAGATION

D. Korte*, T. Hüttl, F. Kennepohl, K. Heinig
MTU Aero Engines GmbH
Dachauer Str. 665, 80995 München

A numerical method has been developed to calculate the noise within a turbine / compressor by means of CFD (Time Linearized Euler Code). The noise generation, caused by the interaction of neighbouring cascades can be calculated as well as the noise propagation within the turbomachine. Numerical results obtained by this method are compared to measurements. The CFD results are in good agreement with the measurements. Especially the cut-on, cut-off behaviour of the modes in the duct is simulated successfully.

1. INTRODUCTION

Within the European research project TurboNoiseCFD, a methodology has been developed to calculate the tonal sound generation due to aeroacoustic interaction as well as the propagation of tonal sound through multistage turbomachines. Three rotor-stator interaction mechanisms are considered: wake interference and upstream and downstream interference of the steady pressure field fixed to a cascade, interacting with a neighbouring blade row [3].

The numerical method is based on the time linearized Euler code Lin3D for 3D cascade flows, developed at MTU. The unsteady flow is assumed to be a small harmonic perturbation of the non-linear steady flow, so that the steady flow problem is decoupled from the unsteady problem. As long as the wave amplitudes remain moderate, the higher order terms in the governing equations derived under this assumption can be neglected and the describing unsteady flow equations become linear. The small-disturbance Euler equations are transformed into the frequency domain, so that the results are given as amplitudes and phases of the flow variables in the whole (3D) computational domain. Lin3D is already used for aeroelastic design of aeroengine compressors and turbines [8,9,10]. The code and its extension to multistage calculations has also been tested for various aeroacoustic applications, ranging from simplified flat plate test cases to realistic single- or multistage turbomachines [1,2,6,7,11].

The focus of the present study is a new method to calculate noise propagation within a turbomachine.

2. TEST CASE

The test case of the present investigation is a three-stage low pressure turbine, for which measurements have been performed by DLR within the earlier EC project "RESOUND", see FIG. 1

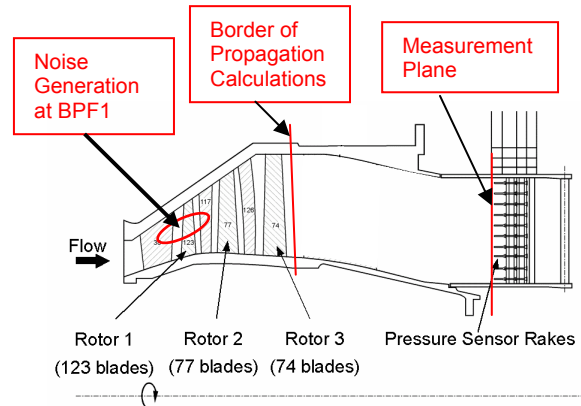


FIG. 1 RESOUND turbine, a 3-stage LP turbine

Measurements have been performed within the RESOUND programme for configurations with and without exit guide vane (EGV). The data used for a comparison with the numerical results in this report were measured without EGV.

The pressure sensors for the noise measurements are placed downstream of the turbine (see FIG.1). Numerically, the noise propagation was only calculated up to the exit of *Rotor 3*. The different position with respect to the measurement plane has to be taken into account when comparing numerical data and measurement data, especially because the radius decays from calculation plane (exit of *Rotor 3*) to measurement plane.

The calculations were performed for the configuration without exit guide vanes at 74% design speed.

3. NUMERICAL RESULTS

3.1. Generated Sound

The sound generation mechanism assumed to be dominant, is the interaction between neighbouring cascades. Due to the interactions, tones at the blade passing frequencies (BPF) are generated. At each cascade (stator or rotor) tones can be generated due to one of the following disturbances, caused by a neighbouring cascade, leading to an unsteady loading of the vanes (blades):

- steady pressure field („potential field“) of upstream cascade, rotating relatively to the considered cascade
- steady pressure field („potential field“) of

* Email: Detlef.Korte@muc.mtu.de

downstream cascade, rotating relatively to the considered cascade

- c) viscous wake of upstream cascade, rotating relatively to the considered cascade

In the calculations presented here, only these mechanisms are taken into account. Each interaction (a, b and c) is treated separately during the simulation process.

Noise is generated and radiated into upstream and downstream flow direction. Accordingly, for each interaction pair of cascades, the upstream and downstream sound is calculated. Only tones below 10 kHz were calculated: $BPF_1(123)$, $BPF_2(77)$, $BPF_3(74)$, $2BPF_2(77)$, $2BPF_3(74)$. The calculations are performed on the finest of three computational meshes.

Each calculation results in a sound power level distribution of azimuthal modes. Because of the different interaction mechanisms of neighbouring cascades, treated in separate calculations, at one azimuthal mode there can be up to 3 different values for one azimuthal modal sound power level.

The sound power spectra of the sound waves with frequency BPF_1 , travelling in upstream (FIG. 2) and downstream direction (FIG. 3) are presented here as examples of the obtained results.

It turns out, that for each frequency the sound power of up to five modes is clearly higher than the sound power of the others. These are the important modes with respect to noise investigations.

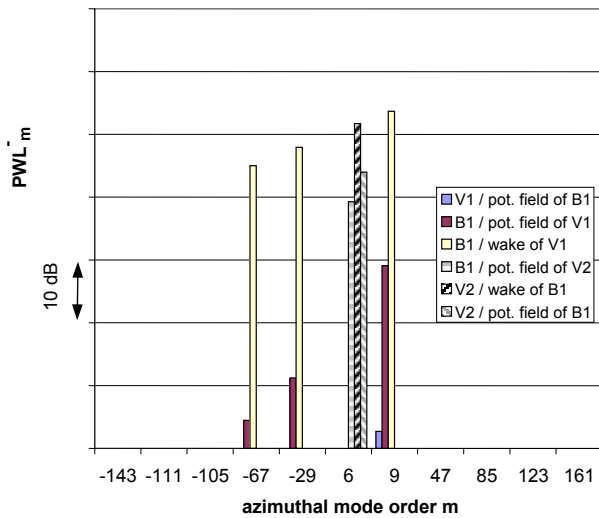


FIG. 2 Sound Power Spectrum $BPF_1(123)$ at location of noise generation, upstream travelling sound waves

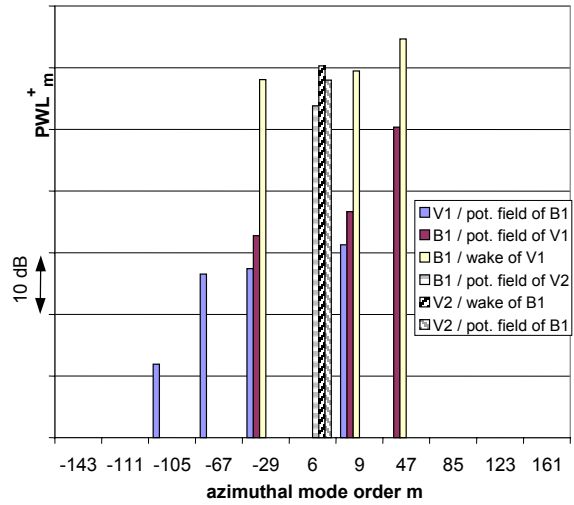


FIG. 3 Sound Power Spectrum $BPF_1(123)$ at location of noise generation, downstream travelling sound waves

3.2. Propagated Sound

It is not only important to know the sound power at its origin but also at the exit of the turbine. Since no exit guide vane was present in the here investigated case, to save computational time and because of numerical dissipation, it was decided to calculate the propagation of sound only up to the exit of *Rotor 3* instead of calculating it up to the exit of the turbine (FIG.1).

The chosen method (“beetle method”) was a simple perturbation propagation: For each relevant circumferential mode, the downstream (upstream) travelling pressure perturbation at the outlet (inlet) of one calculation is used as the inlet (outlet) perturbation of the downstream (upstream) following grid, after a transformation to the cascade’s frame of reference. A decomposition into radial modes is unnecessary.

The sound propagation of the three blade passing frequencies was calculated. Only straightforward sound propagation calculations in flow direction have been performed. No reflections or upstream propagation was considered. Scattered modes were ignored for this investigation. The calculations have been performed on the medium size mesh out of three meshes.

As an example, the propagation of the relevant modes of the first blade passing frequency (BPF_1) is presented in FIG. 4. The legend of FIG. 4 contains the following information: mode order; location of sound generation; mechanism of sound generation.

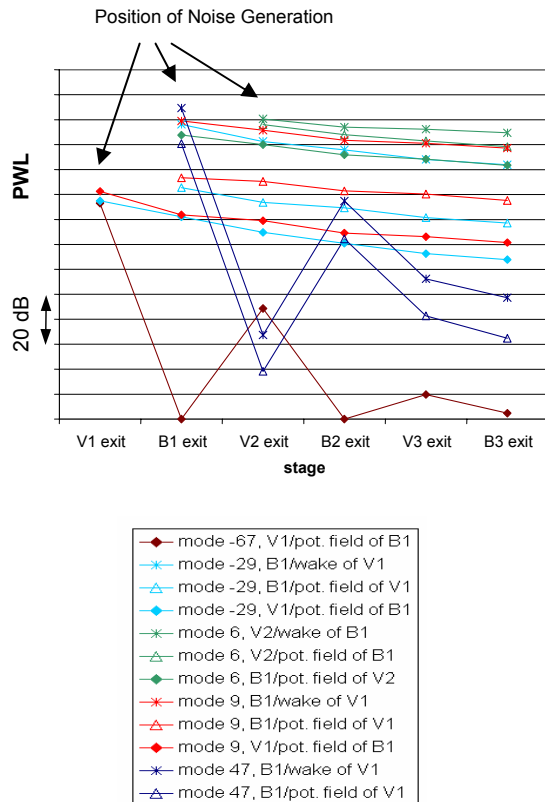


FIG. 4 Sound propagation – CFD Results for BPF₁

The generated modal sound power levels were presented in FIG. 3. For these modes ($m=-67, -29, +6, +9, +47$) sound propagation calculations have been performed up to the exit of *Rotor 3*. The resulting modal sound power levels at the exit of each cascade are presented in FIG. 4. The most left point of each curve denotes the sound power at the generation origin.

Two different effects can be observed. On the one hand there are modes that remain cut-on at all cascades ($m=-29, +6, +9$); on the other hand there are modes that switch between cut-on and cut-off ($m=-67, +47$).

The sound power of the cut-on modes ($m=-29, +6, +9$) decays monotonically from the sound generation origin to the last cascade.

The sound powers of the other modes ($m=-67, +47$) are represented by zigzag lines in FIG. 4. One cascade downstream of their generation origin they become cut-off, in the next stage cut-on and then cut-off again up to the exit of *Rotor 3*.

The pressure disturbance amplitude decays monotonically from cascade to cascade but while the phase difference to the sound particle velocity is approximately 90° when the respective mode is cut-off, pressure disturbance and sound particle velocity are almost in phase for a cut-on mode.

The increase in sound power from one cascade to the next, related to a change from cut-off to cut-on, is an effect that can be looked on as a sound generation process: The

disturbance pressure field of an upstream cut-off mode can interact with the steady pressure field of the downstream cascade and thus noise can be generated, just as in the case of the potential field interaction, described in chapter 3.1.

4. COMPARISON CFD VS. MEASUREMENT

4.1. CFD Results at Generation Origin vs. Measurement at Downstream Position

In this chapter, a comparison between the measured values and the calculated sound power values at source is presented to show that propagation effects cannot be neglected.

In FIG. 5 the calculated modal sound power levels are compared with the measured values. The diagram on the left hand side shows the calculated sound power levels of the frequency BPF₁ at the sound generation location. The diagram on the right hand side shows the respective measured sound power levels of the same frequency BPF₁, downstream of the turbine.

The modal sound power levels of FIG. 5-a are the result of a summary of the sound power levels presented in FIG. 3, in the sense that the sound powers of the same azimuthal mode order, but generated due to different mechanisms, are summed up. For this summation it was assumed that modes of the same order, but generated due to the different mechanisms, are in phase. Thus, a „worst case“ value of the radiated noise is calculated for each azimuthal mode.

Only a few modes of noise generation calculations and measurements correspond to each other. These corresponding modes are marked in FIG. 5. While measured values exist for a limited, but predominantly continuous, range of azimuthal mode orders, calculated values exist only for some discrete mode orders, generated by the interaction of neighbouring cascades.

Sound power levels below 60 dB are not considered important and consequently not presented below. Values up to this limit can be the result of numerical effects during calculations.

Comparing measurement and calculation values of the sound power level of one mode, three important cases can be observed:

- 1) the modal sound power level exists in both cases and its value exceeds the lower limit, specified above (>60 dB)
- 2) the modal sound power level does not exist in case of the calculation; the modal sound power level exists in case of the measurement and exceeds the lower limit, specified above (>60 dB).
- 3) the modal sound power level exists in case of the calculation and exceeds the lower limit, specified above (>60 dB); the modal sound power level does not exist in case of the measurement or is below the limit (<60 dB)

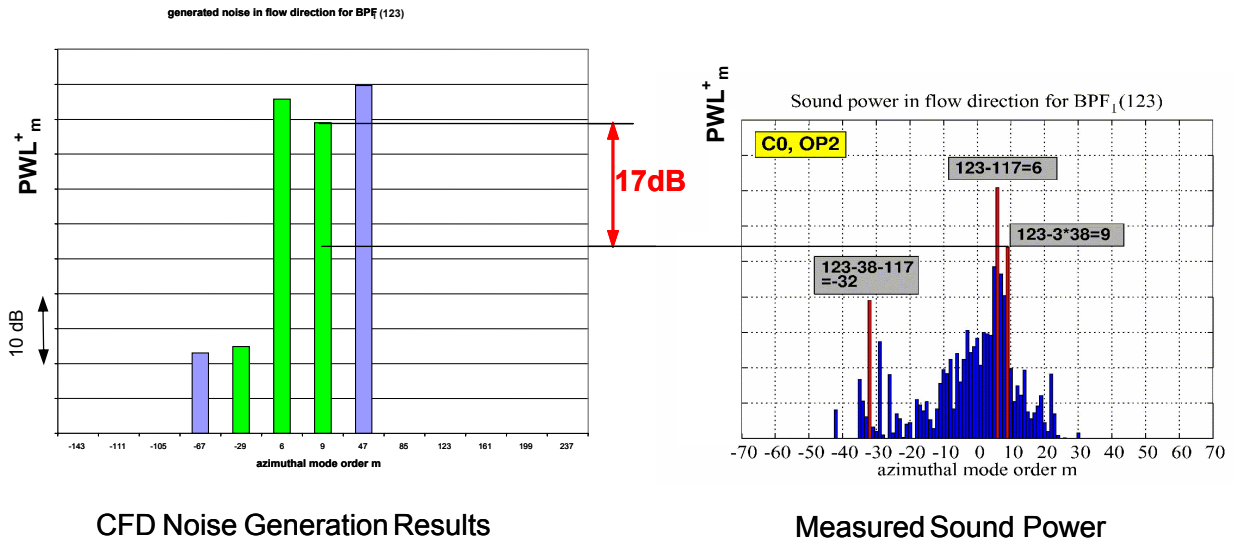


FIG. 5 a) CFD Results for Sound Power Spectrum (BPF₁) at Generation Origin

b) Measured Sound Power Spectrum (BPF₁) downstream

Considering these three cases the following can be stated concerning the BPF₁ results:

ad 1) The three modes of the orders $m = -29, +6, +9$ exist as well in the noise generation calculations, as in the downstream measurement results (FIG. 5). They are marked by green colour in FIG. 5-a and arrows in FIG. 5-b. Accordingly it is assumed that the calculated modes of the orders $m = -29, +6, +9$ will be propagated (cut-on) up to the measurement plane. This is shown to be true (at least up to the exit of *Rotor 3*) in FIG. 4. In the measurement, the sound power levels of the three common modes are high, relative to values of similar mode orders. Thus, one can clearly see peaks in FIG. 5-b at these mode orders. This indicates the importance of the noise generation mechanism exclusively investigated in the calculations, the interaction of neighbouring cascades. Nevertheless, the difference of the absolute values, eg. 17 dB in case of mode order $m = +9$, is very high when the measurement is compared to the calculated results at source only. Beyond that, the difference in case of mode $m=+9$ varies strongly from the difference in case of mode $m=-29$ and the one in case of mode order $m=+6$. The last two topics indicate the importance of the propagation effects. These cannot be neglected.

ad 2) The existence of peaks, like the one for mode order $m = -32$ in the measurement spectrum, FIG. 5-b (no correspondence in the calculation spectrum, FIG. 5-a), shows that other noise generation mechanisms, as for example the interaction of three cascades, can be important too. These are not modelled numerically.

ad 3) A peak in the generation spectrum, FIG. 5-a, without a corresponding one in the measurement spectrum, FIG. 5-b, leads to the assumption, that this mode will change to cut-off during the propagation calculation from the noise generation origin to the measurement plane. The highest peak of such a mode corresponds to the order $m = 47$ (see FIG. 5-a). The

measured modal value is very low, such that it is not even visible in FIG. 5-b. In FIG. 4 it is shown that mode 47 indeed becomes cut-off during the propagation calculation.

Investigations of the other blade passing frequencies show similar behaviour.

4.2. CFD Results of Sound Propagation to *Rotor 3* Exit vs. Measurement at Downstream Position

In this part the sound power levels of the BPF₁ modes, propagated to the *Rotor 3* exit, are compared to experimental values, measured further downstream.

The relevant modes from the noise generation calculations have been used to start noise propagation calculations up to the exit of *Rotor 3*. This is not the measurement plane. Propagation calculations up to the measurement plane have not been conducted. No reflection was considered, only straightforward propagation of the disturbance modes was conducted.

Five modes of the frequency BPF₁ have been propagated straightforward. During the process, parts of the sound power of a specific mode and frequency are transferred to other modes and frequencies. The evaluation within this chapter considers only the sound power, related to the original disturbance mode and frequency.

In section 3.2 the results of the propagation calculations of these modes ($m=-67, -29, 6, 9, 47$) were presented. In this part they are compared to measured values. The results of the comparison of the modes generated due to different mechanisms are presented in FIG. 6. The sound powers of the same azimuthal mode order, but generated due to

different mechanisms, are summed up and compared to the measured values in FIG. 7. A blue bar denotes the calculated-generated noise, a red bar the calculated-propagated noise and a yellow bar the measured sound.

The sound of *mode -67* is generated at *stator 1*, due to the pressure field of *rotor 1* (see FIG. 3). The sound propagation calculations were presented in FIG. 4. The calculated sound power level at the exit of *Rotor 3* is compared to the measured value in FIG. 6-a and FIG. 7.

The sound of *mode -29* is generated due to three mechanisms: at *Stator 1*, due to the pressure field of *rotor 1*; at *Rotor 1* due to wake and pressure field of *Stator 1* (see FIG. 3). The sound propagation calculations of all three disturbances were presented in FIG. 4. The calculated sound power levels at the exit of *Rotor 3* are compared to the measured value in FIG. 6-b. The resulting total sound power level of *mode -29* at the exit of *Rotor 3* is compared to the measured value in FIG. 7.

Three mechanisms of noise generation lead to a sound mode of order $m = 6$. Two of them are generated at *Stator 2*, one due to the wake of *Rotor 1*, the other due to the pressure field of *Rotor 1*. The third is generated at *Rotor 1*, due to pressure field of *Stator 2* (see FIG. 3). All of them were selected as disturbances for propagation calculations (see FIG. 4). The comparison of the propagation results to the measured value is presented in FIG. 6-c. The resulting total sound power level of *mode 6* at the exit of *Rotor 3* is compared to the measured value in FIG. 7.

Three mechanisms of noise lead to a sound mode of order $m = 9$ (see FIG. 3): noise generation at *Stator 1*, due to the pressure field of *Rotor 1*; noise generation at *Rotor 1* due to wake and pressure field of *Stator 1* (see FIG. 3). Although one of them is clearly dominant, all were selected as disturbances for propagation calculations (see FIG. 4). The comparison to the measured value is presented in FIG. 6-d. The resulting total sound power level of *mode 9* at the exit of *Rotor 3* is compared to the measured value in FIG. 7.

Two mechanisms of noise generation lead to a sound mode of order $m = 47$ (see FIG. 3). Both of them were selected as disturbances for propagation calculations (see FIG. 4): both tones are generated at *Rotor 1*, one due to the pressure field of *Stator 1*, the other due to the wake of *Stator 1*. The comparison to the measured value is presented in FIG. 6-e. The resulting total sound power level of *mode 47* at the exit of *Rotor 3* is compared to the measured value in FIG. 7.

Except for *mode -67*, the calculated sound power level at the exit of *Rotor 3* is always slightly greater than the measured one. The calculated value for *mode -67* is much lower than the measured one. Nevertheless it is at least qualitatively in accordance with the calculated one, since it is low with respect to measured sound powers of other modes (see FIG. 7).

The measured sound power level of *mode 6* is the highest of all modes while the measured value of *mode 47* is the lowest of all considered five modes. In contrast, both noise generation calculations lead to noise levels in the same range. It is shown in FIG. 6-c,e and FIG. 7 that the sound

power levels of these modes, after propagating them to the exit of *Rotor 3*, match well with the measured values. It was shown in FIG. 4 that the sound power of *mode 6* decays during the propagation, but the mode remains cut-on. It was also shown that *mode 47* becomes cut-off at the exit of *Rotor 3*. Accordingly its sound power decays nearly to zero. This corresponds to the low measured value.

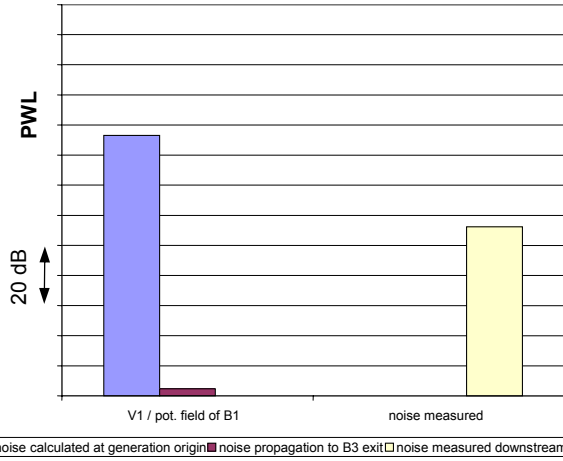
The behaviour of the modes $m = -29, +9$ was shown to be analogue to *mode 6* (see FIG. 4). The sound power decays monotonic from one stage to the next. At the exit of *Rotor 3*, the sound power level matches good with the measured value in case of *mode 9* (see FIG. 6-d and FIG. 7).

The behaviour of mode $m = -67$ was shown to be analogue to *mode 47* (see FIG. 4). It becomes cut-off at the exit of *Rotor 3*, which is related to a sound power level near zero.

Another interesting effect observed, when doing a propagation calculation with the presented method, is the mode scattering in circumferential and radial order. This is illustrated at the example of *mode 6*, generated at *Stator 2* and prescribed as a disturbance at the following cascade, *Rotor 2* (FIG. 8). Apart from the sound pressure at *mode 6*, high sound pressures occur at the azimuthal mode order $m = +83$, a lot less at other mode orders (azimuthal mode scattering). Beyond that, the radial decomposition of *mode 6* leads to different results at the entrance (disturbance) and the exit of the grid (radial mode scattering).

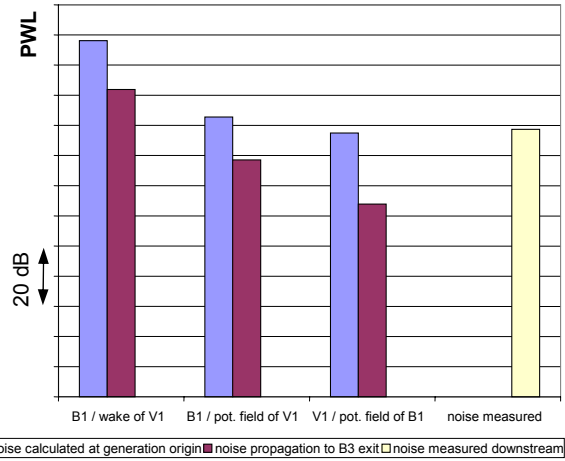
The effects of mode scattering can be very different for different circumferential modes. While for one mode almost no sound power is shifted, almost the total sound power can be transferred in other cases. This is shown in FIG. 9. *Mode 6* and *mode 47*, both generated at *Rotor 1*, are prescribed as pressure disturbances at the entrance of *Stator 2*. The scattering effects, when propagating *mode 6*, are minimal. In case of *mode 47* a different behaviour can be observed: most of the sound power is transferred to *mode -70*, which is cut-on at the exit of *Stator 2*, while *mode 47* becomes cut-off.

BPF1, mode -67: calculation vs. measurement



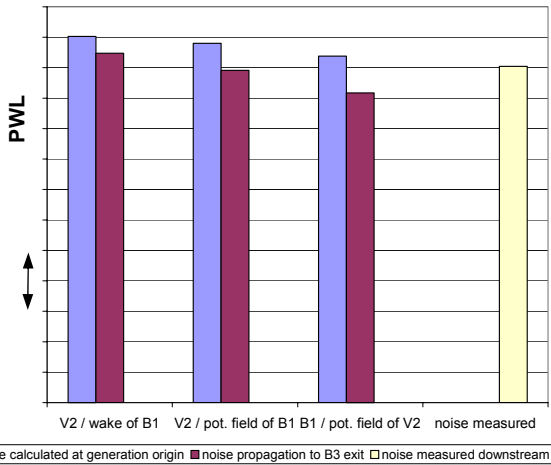
(a) mode: -67

BPF1, mode -29: calculation vs. measurement



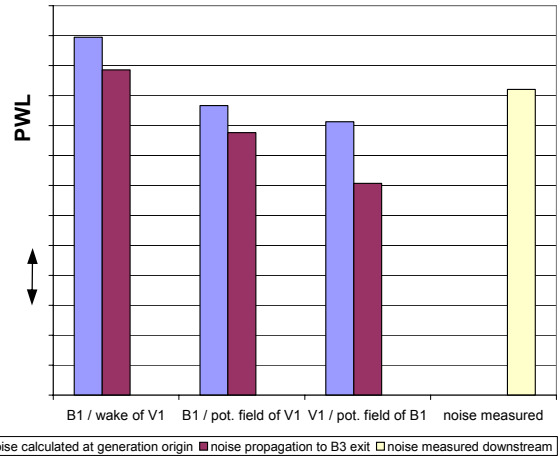
(b) mode: -29

BPF1, mode 6: calculation vs. measurement



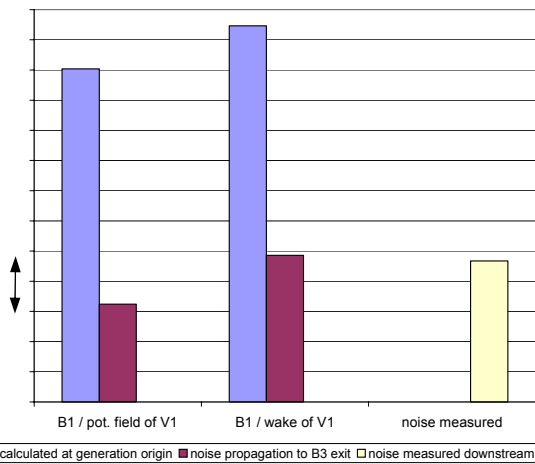
(c) mode: 6

BPF1, mode 9: calculation vs. measurement



(d) mode: 9

BPF1, mode 47: calculation vs. measurement



(e) mode: 47

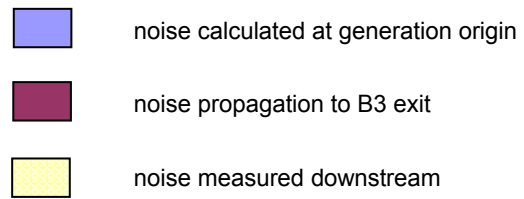


FIG. 6 Sound Power Levels for BPF1 – modes: -67, -29, 6, 9, 47 – calculated propagation vs. measurement

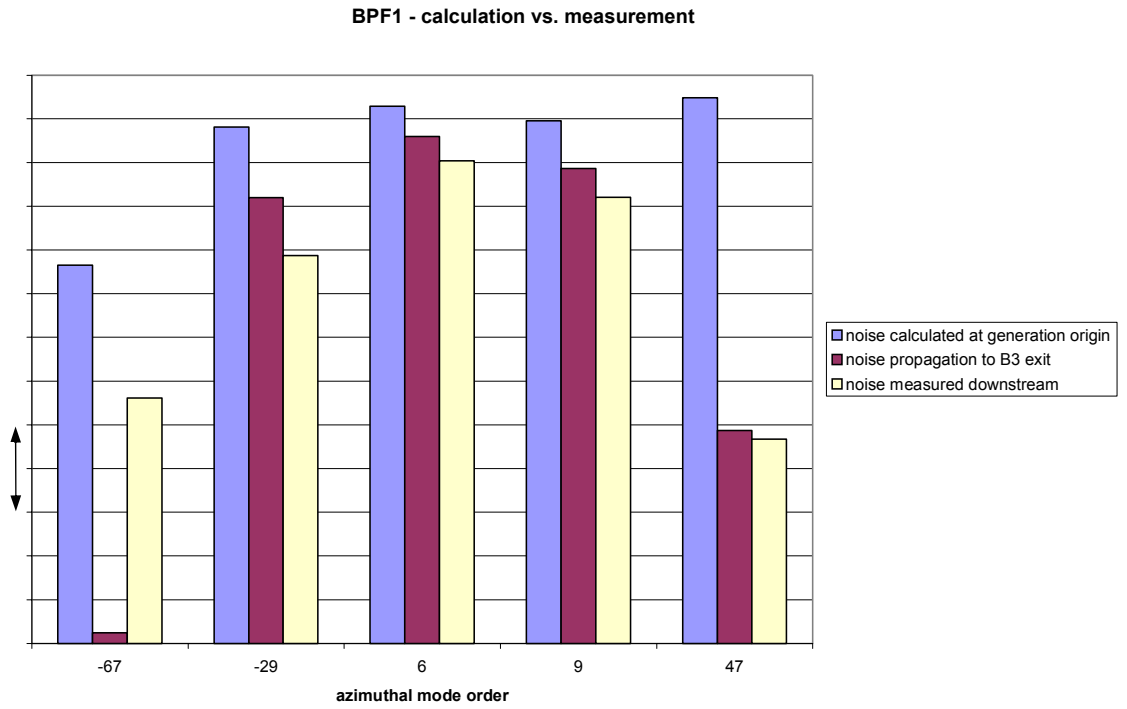


FIG. 7 BPF1 – Spectrum of Modal Sound Powers – Calculation vs. Measurement

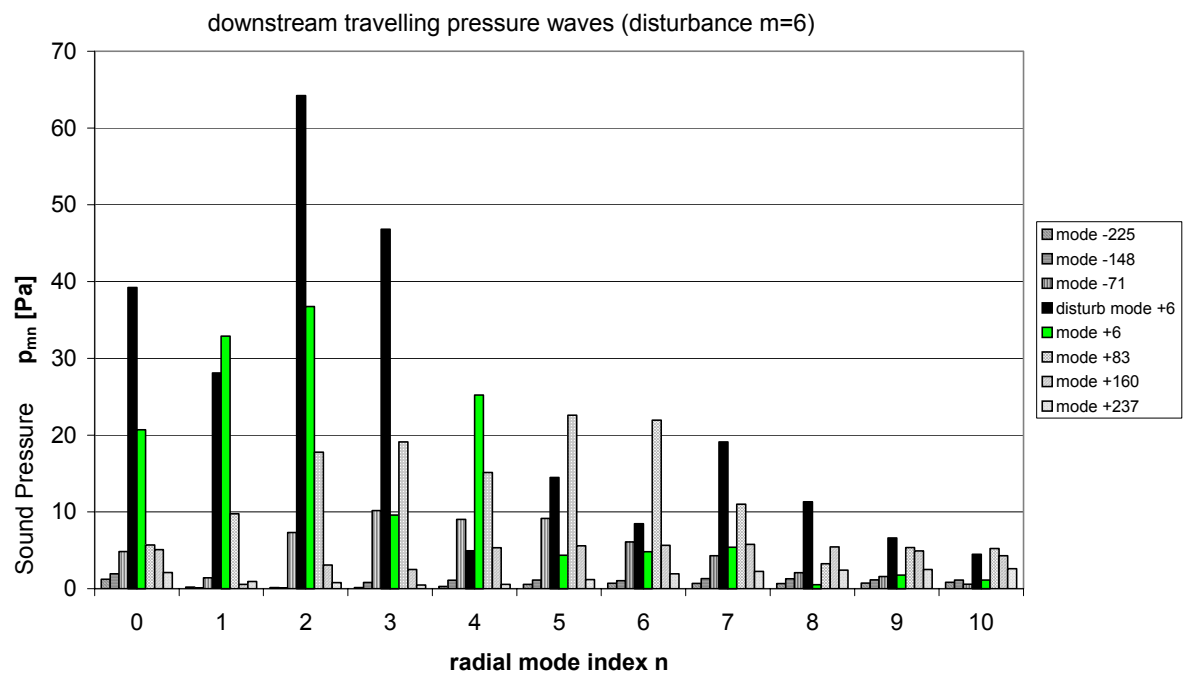


FIG. 8 Circumferential and Radial Scattering at Rotor 2 of mode $m = +6$ (generated at Stator 2); disturbance mode at entry of Rotor 2, all other values at exit of Rotor 2

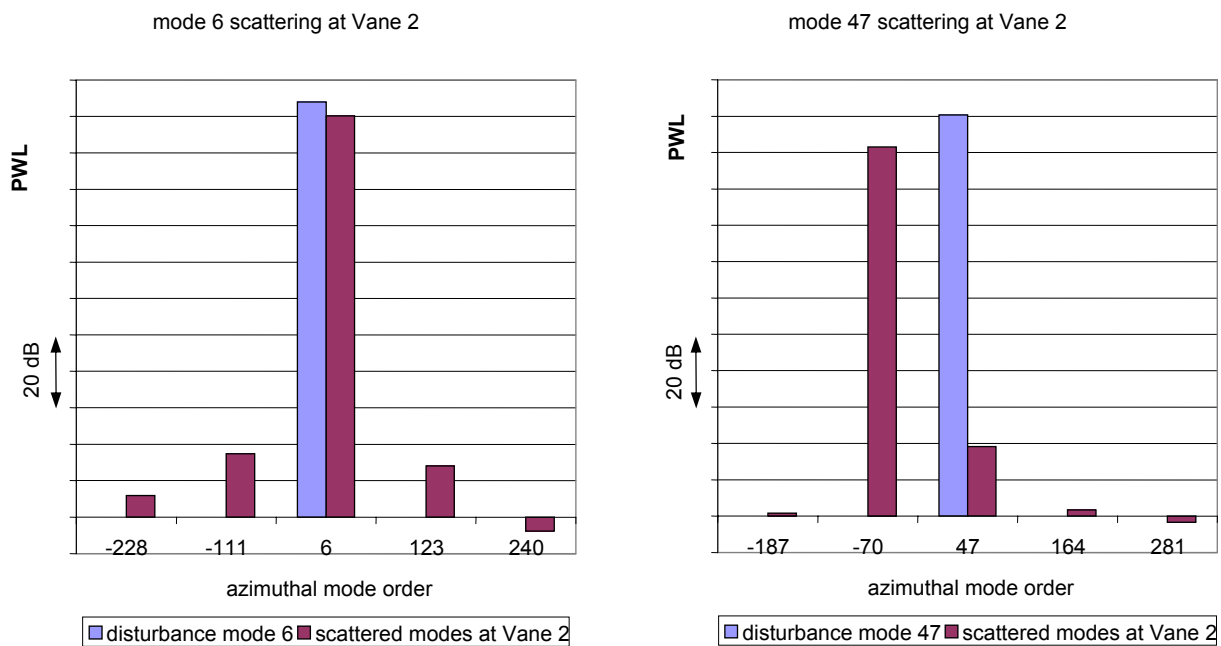


FIG. 9 Circumferential Mode Scattering

5. CONCLUSION

The noise of a turbine has been calculated by means of CFD. This paper presents the results of noise generation and propagation calculations with a linearized Euler code (Lin3D). These results are compared with measured data, delivered by DLR. Consistencies and differences between simulation and measurement are described.

The CFD calculations consider the noise generation by the interaction of two neighbouring cascades. The comparison of numerical results and measured data shows that this noise generation mechanism is indeed very important. But it also shows that other mechanisms should not be neglected. One of such mechanisms is the interaction of three cascades.

In this report it was shown that it is important to perform the noise propagation calculations up to the last stage, even if a mode becomes cut-off at an intermediate stage. It was shown that it can become cut-on again.

To propagate the sound of a mode from one cascade to the next, its pressure disturbance evaluated in the upstream cascade exit was prescribed at the inlet of the investigated grid ('Beetle Method'). Such a disturbance pressure field does also exist in case of a cut-off mode. Its amplitude would decay to zero over some distance but in case of the RESOUND turbine the stages are very close together.

The propagation of a cut-off mode can also be looked at as a noise generation process: The steady pressure field of the investigated cascade interacts with the relatively rotating disturbance pressure field and such generates tones, just as in the potential field interaction process. The calculated sound power of a mode, which is cut-on at the exit of the last stage, seems to be reasonable, even if the

mode was cut-off at an intermediate stage.

While another tested method of sound propagation [12], the four pole theory [4,5], is exact under certain circumstances (e.g. no mode conversion), the beetle method leads to best results when any reflection of waves can be neglected. In practice, reflection of waves could become very relevant for multistage turbomachines. But this was not the case here.

Phenomena of an infinite number of reflections of sound waves between two cascades can be important. In that case, the propagation of a single sound mode depends on the axial gap between two cascades and the sound can be amplified or extinguished when superposing the sound waves.

A first improvement of the beetle method could be to consider at turbine (compressor) cases the first reflection of the upstream (downstream) propagating sound at the neighbouring cascade. Then, unreflected downstream (upstream) propagating sound and reflected downstream (upstream) propagation sound has to be superposed.

Comparing the absolute sound power values, resulting from simulation respective measurement, the following uncertainties have to be considered: The position of the plane, up to which the noise propagation was calculated, is different from the measurement plane. In case of the simulation, one mode can be created by different disturbances (wake, potential pressure field interaction). To calculate the resulting sound power level, the phase relation would have to be considered. For this investigation, this was done by a worst case consideration.

6. ACKNOWLEDGEMENT

The support of the DLR, who provided the evaluated measurement results, is gratefully acknowledged.

The work described in this paper has been carried out in the framework of the research project 'Turbomachinery noise source CFD models for low noise aircraft designs - TurboNoiseCFD' funded by the European Commission within the GROWTH - 5th framework programme.

7. REFERENCES

- [1] Gautier, S.: Aero-acoustic analysis of a multistage turbine. Diploma thesis, EPFL – MTU Aero Engines GmbH, München Feb. 2002
- [2] Gautier, S., Hüttl, T., Kennepohl, F.: Aeroacoustic Analysis of Multistage Turbines, German Aerospace Conference, Stuttgart 2002.
- [3] Hall, K.C. and Silkowski, P.D.: "The influence of neighboring blade rows on the unsteady aerodynamic response of cascades", ASME-paper 95-GT-35, presented at the International Gas Turbine and Aeroengine Congress & Exposition Houston, Texas - June 5-8, 1995.
- [4] Heinig, K.E.: "Sound Propagation in Multi-Stage Axial Flow Turbomachines", AIAA 7th Aeroacoustics Conference, Oct. 5-7, 1981, Palo Alto, California, AIAA-Paper AIAA-81-2047, 1981.
- [5] Heinig, K.: "Ein Beitrag zur Berechnung der Schallemission mehrstufiger Verdichter und Turbinen von Flugzeugtriebwerken", Dissertation, TU Berlin, 1994.
- [6] Hüttl, T., Kahl, G., Kennepohl, F. and Heinig, K.: Resolution Requirements for the Numerical Computation of Tonal Noise in Compressors and Turbines of Aeroengines, NATO RTO/AVT Symposium on Aging Mechanisms and Control, Part A - Development in Computational Aero- and Hydro-Acoustics, 8-11 October 2001, Manchester, UK.
- [7] Hüttl, T., Kennepohl, F., Kahl, G., Heinig, K.: „Computation of rotor-stator interaction noise generation using a linearized Euler method“, presented at the 5th CEAS-ASC Workshop on Turbomachinery Noise and Duct Acoustics, 8-9 November 2001, Eindhoven University of Technology, The Netherlands
- [8] Kahl, G.: Application of the Time Linearized Euler Method to Flutter and Forced Response Problems, ASME-95-GT-123, 1995.
- [9] Kahl, G. and Klose, A.: Time Linearized Euler Calculations for Unsteady Quasi-3D Cascade Flows, *6th Symp. on Unsteady Aerodynamics and Aeroelasticity in Turbomachines and Propellers*, Notre Dame, IN, Sept. 15-19, 1991.
- [10] Kahl, G. and Klose, A.: Computation of Time Linearized Transonic Flow in Oscillating Cascades, *Int. Gas Turbine and Aeroengine Congress and Exposition*, Cincinnati, Ohio - May 24-27, ASME-93-GT-269, 1993.
- [11] Kennepohl, F., Kahl, G., Heinig, K.: „Turbine blade/vane interaction noise: calculation with a 3D time-linearised Euler method“, AIAA-2001-2152
- [12] Uslu, S., Hüttl, T., Heinig, K.: Simulation of Noise Generation due to Blade Row Interaction in a High Speed Compressor, German Aerospace Conference, Stuttgart 2002.